JACS
JOURNAL OF THE AMERICAN CHEMICAL SOCIETY

Article

pubs.acs.org/JACS

Crystallization and Interconversions of Vapor-Sensitive, Luminescent Polymorphs of $[(C_6H_{11}NC)_2Au^I](AsF_6)$ and $[(C_6H_{11}NC)_2Au^I](PF_6)$

Mark A. Malwitz, Sang Ho Lim, Rochelle L. White-Morris, David M. Pham, Marilyn M. Olmstead, and Alan L. Balch*

Department of Chemistry, University of California, Davis, California 95616, United States

Supporting Information

ABSTRACT: The remarkable, vapor-induced transformation of the yellow polymorphs of $[(C_6H_{11}NC)_2Au^I](AsF_6)$ and $[(C_6H_{11}NC)_2Au^I](PF_6)$ into the colorless forms are reported along with related studies of the crystallization of these polymorphs. Although the interconversion of these polymorphs is produced by vapor exposure, *molecules of the vapor are not incorporated into the crystals*. Thus, our observations may have broad implications regarding the formation and persistence of other crystal polymorphs where issues of stability and reproducibility of formation exist. Crystallographic studies show that the colorless polymorphs, which display blue luminescence, are isostructural and consist of linear chains of gold(I) cations that self-associate through aurophilic interactions. Significantly, the yellow polymorph of $[(C_6H_{11}NC)_2Au^I](AsF_6)$ is not isostructural with the yellow polymorph of $[(C_6H_{11}NC)_2Au^I](PF_6)$. Both yellow polymorphs exhibit green emission and have the gold cations arranged into somewhat bent chains with significantly closer Au···Au separations than are seen in the colorless counterparts. Luminescence differences in these polymorphs clearly enhance the ability to detect and monitor their phase stability.

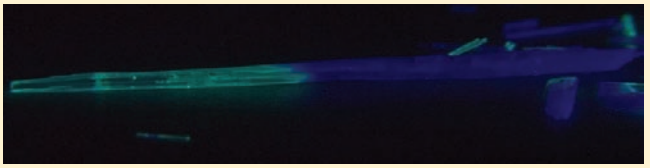

INTRODUCTION

A number of transition metal complexes undergo changes in color or luminescence upon exposure to volatile organic compounds. Such complexes provide the basis for the development of a range of chemosensors.[1−3] These sensing processes, known as vapochromism or vapoluminescence, invariably result in the uptake of the volatile organic compound into the solid to produce a change in its structure. For example, a number of metal chain complexes such as $\{Tl[Au(C_6Cl_5)_2]\}_n$ are vapochromic as a result of uptake of the volatile compounds, which coordinate to the metal ions in the chain and alter the interactions between the metal ions.[4−8] Several planar Pt(II) complexes, e.g., the double salts, $[Pt(CNAr)_4][Pt(CN)_4]$, form columns in the solid state with extended ···Pt···Pt···Pt··· interactions.[9−15] These salts can display reversible, vapor-induced color changes, which result from absorption of solvent molecules that alter the nature of the ···Pt···Pt···Pt··· interactions particularly through the formation of hydrogen bonds with the cyano ligands. Some metal hydrazone complexes of iron(II), palladium(II), and platinum(II) show vapochromic behavior that results from the alteration of the hydrogen bonding within the supramolecular structures of the complexes due to the adsorption of the vapor.[16,17] Polymeric $\{Cu^I(4\text{-picoline})I\}_n$, which shows a blue luminescence (λ_{max} = 437 nm), is transformed into the discrete tetrameric, yellow luminescent (λ_{max} = 580 nm) $\{Cu^I(4\text{-picoline})I\}_4\cdot 2(\text{toluene})$ upon exposure to toluene as vapor or liquid.[18,19] The process is reversed by exposure of $\{Cu^I(4\text{-picoline})I\}_4\cdot 2(\text{toluene})$ to pentane vapor or to vacuum.

Many colorless, nonluminescent, two-coordinate gold(I) complexes undergo self-association upon crystallization to produce luminescent solids.[20] Aurophilic interactions,[21,22] attractive forces between gold ions with bond energies of ca. 7−11 kcal/mol, are an integral component of the self-association. Since the interactions between the individual gold(I) monomers are relatively weak, crystallization of these gold complexes is frequently accompanied by the formation of polymorphs that can differ in the nature of the aurophilic interactions and in the luminescence. Polymorphs are isomers at the individual crystal level in which the same molecule or salt crystallizes in different fashions, which results in differences in space group and cell dimensions.[23,24] In general, these polymorphs differ in such factors as the packing of the molecules and their relative orientation within the crystal, the conformations of the molecules, and the degree of ordering for highly symmetric molecules.[25,26] In such cases, the physical properties of the polymorph reflect the individual molecular character. However, when there are significant electronic interactions between the components that change in different polymorphs, there can be important changes in their properties.[27] For example, 4,4′,5,5′-tetramethyl-delta-2,2′-bi-1,3-diselenole-7,7,8,8-tetracyano-*p*-quinodimethane (TMTSF·TCNQ) forms two polymorphs.[28,29] The red form is a semiconductor that involves a mixed stack of donor and acceptor molecules, while the black polymorph is a conductor that crystallizes with segregated stacks of donors and acceptors. These observations

Received: February 29, 2012
Published: April 17, 2012

proved the importance of segregated stacks in producing electrical conductivity in organic donor−acceptor co-crystals. Polymorph formation is a particularly challenging issue in the pharmaceutical industry, since many drugs are formulated as solids.[30,31] Changes in the physical properties, such as solubility, of those solids can alter their potency, as was the case with ritonavir (sold as Norvir), an HIV protease inhibitor.[32]

Polymorph formation of gold(I) complexes frequently results in marked changes in spectroscopic properties, particularly luminescence that is influenced by aurophilic interactions. Examples of gold(I) complexes that occur as polymorphs include the yellow and colorless forms of $[(C_6H_{11}NC)_2Au^I](PF_6)$, in which the cations crystallize in extended columns with shorter Au···Au separations in the yellow form.[33] (Ph_2MeP)-AuCl crystallizes in dimeric and trimeric forms with distinct luminescence for each form.[34−36] Leznoff and co-workers have identified polymorphs of polymeric $Cu[Au(CN)_2]_2(DMSO)_2$ which differ in their copper coordination.[37] Similarly, $Zn[Au(CN)_2]_2$ crystallizes in four polymorphic forms, three of which are luminescent.[38] The solvoluminescent complex, $\{Au(MeOC{=}NMe)\}_3$, also forms polymorphs.[39] The solvoluminescent form crystallizes with prismatic columns in the hexagonal space group *P6/m*. This complex also forms non-solvoluminescent crystals in a triclinic form and a monoclinic form that lack the columnar stacking seen in the hexagonal form. A related trinuclear complex, $\{Au(MeOC{=}N\text{-}n\text{-}pentyl)\}_3$, forms two polymorphs which also differ in the nature of the aurophilic interactions between the molecules.[39] Crystals of $[\mu_3\text{-}S(Au^ICNC_7H_{13})_3](SbF_6)$ undergo a polymorphic phase change upon cooling that produces lengthening of the aurophilic interactions between one pair of cations, while inducing shortening of the aurophilic contacts between the other pair of cations. Changes in the luminescence of the clusters accompany the phase change.[40] Some $Au^I_3Cu^I_2$ alkynyl clusters form polymorphs that display green or orange luminescence.[41] Crystals of $Au_2(\mu\text{-dpae})X_2$ (dpae = bis-(diphenylarsino)ethane; X = Cl, Br, or I) form dimorphs. The α-form crystallizes as colorless blocks in which individual molecules of $Au_2(\mu\text{-dpae})X_2$ form discrete dimers through close Au···Au contacts, while the β-form exists as colorless needles with the $Au_2(\mu\text{-dpae})X_2$ molecules assembled into polymeric chains through aurophilic interactions.[42]

Aurophilic interactions can also produce luminescent crystals that are responsive to changes in their environment.[20,36] In particular, many gold crystalline complexes display solvo- or vapoluminescence that is a result of uptake of the vapor into the solid phase. Thus, the binuclear dithiocarbamate complex, $Au^I_2(S_2CN(n\text{-pentyl})_2$, crystallizes in a colorless, nonluminescent form that contains well-separated, dimeric molecules, but an orange, luminescent form is produced when the colorless solid is exposed to solvent vapors such as dimethyl sulfoxide (DMSO).[43,44] Crystallographic characterization of an orange, luminescent form, $Au^I_2(S_2CN(n\text{-pentyl})_2\cdot DMSO$, shows the crystals contain the uncoordinated DMSO molecule and an extended chain of the dimers with short inter- and intramolecular Au···Au separations of 2.96 and 2.77 Å. In a related vein, the binuclear complex $Au_2(\mu\text{-dppp})(BIT)_2$ (where dppp = bis(diphenylphosphine)propane and BIT = 2-benzimidazolethiol) produces blue luminescence, but that luminescence is quenched when the crystals are exposed to the vapor of trifluoroacetic acid.[45] The acid vapor is absorbed by the crystals, and the nature of the aurophilic interactions within the crystals is altered. Treatment of the crystals with triethylamine reverses the process and restores the luminescence. Exposure of the polymorphs of $Zn[Au(CN)_2]_2$ to ammonia vapor results in the alteration in the luminescence and the formation of $Zn(NH_3)_n[Au(CN)_2]_2$ with n = 2 or 4.[38] Similarly, the polymorphs of $Cu[Au(CN)_2]_2(DMSO)_2$ display vapochromic behavior that results in the uptake of the organic vapor into the solid.[37]

Here, we report the observation of vapor-induced structural and luminescence changes in $[(C_6H_{11}NC)_2Au^I](PF_6)$ and the newly synthesized $[(C_6H_{11}NC)_2Au^I](AsF_6)$ that do not involve the uptake of the vapor molecules into the solid, and we examine the processes of crystallization of these two salts that are relevant to the effects of vapor on the luminescence and structure of these polymorphs.

RESULTS

The salt $[(C_6H_{11}NC)_2Au^I](AsF_6)$ was prepared using the procedure previously developed for $[(C_6H_{11}NC)_2Au^I](PF_6)$ with the replacement of $(NH_4)(PF_6)$ with $Li(AsF_6)$.[46] Crystals of two different polymorphs (colorless blocks of one, yellow needles of the other) were obtained by crystallization from dichloromethane/diethyl ether mixtures, *vide infra*. The UV/vis spectra of dichloromethane solutions of the two forms are identical [λ_{max}, nm (ε): 216 (9540), 238 (3070), 244 (3390)] and similar to those of dichloromethane solutions of $[(C_6H_{11}NC)_2Au^I](PF_6)$ reported previously.[33] Solutions of $[(C_6H_{11}NC)_2Au^I](AsF_6)$, like those of $[(C_6H_{11}NC)_2Au^I](PF_6)$, are not luminescent. However, each crystalline polymorph shows a distinctive luminescence, as the data in Figure 1 show. The colorless polymorph produces a blue emission, while crystals of the yellow polymorph produce a greenish luminescence. The infrared spectra of the two polymorphs are also similar but show differences in the region of the isocyanide stretching vibration: colorless polymorph, 2270, 2257 cm^{-1}; yellow polymorph, 2262 cm^{-1}.

Structures of the Colorless and Yellow Polymorphs of $[(C_6H_{11}NC)_2Au^I](AsF_6)$ and Comparison with $[(C_6H_{11}NC)_2Au^I](PF_6)$. Crystallographic data for the two polymorphs of $[(C_6H_{11}NC)_2Au^I](AsF_6)$ are compared with those of the two polymorphs of $[(C_6H_{11}NC)_2Au^I](PF_6)$ in Table 1. The colorless polymorph of $[(C_6H_{11}NC)_2Au^I](AsF_6)$, whose structure is illustrated in Figure 2, is isostructural with the colorless polymorph of $[(C_6H_{11}NC)_2Au^I](PF_6)$. Both colorless polymorphs crystallize in the space group $P2_1/c$ with an asymmetric unit that consists of two half-cations with the gold atoms located at centers of symmetry and one anion in a general position. Since each gold atom is located on a center of symmetry, the two isocyanide ligands coordinate gold in a linear fashion. The gold cations aggregate into an infinite linear chain along the crystallographic *a* axis. Within these chains, the Au1···Au2 contact in the $(AsF_6)^-$ salt is 3.1983(8) Å, which is slightly longer than the corresponding separation (3.1822(3) Å) in the colorless polymorph of $[(C_6H_{11}NC)_2Au^I](PF_6)$. Adjacent cations alternate in orientation and form a semi-staggered array. The orientations of the cyclohexyl groups alternate between axial and equatorial as one moves along the chain of cations. Thus, for the cation containing Au1, the isocyano group is located in an axial site on the cyclohexyl ring, while in the cation containing Au2, the isocyano group resides in an equatorial position of the cyclohexyl ring.

Remarkably, the yellow polymorph of $[(C_6H_{11}NC)_2Au^I](AsF_6)$ is not isostructural with the yellow polymorph of

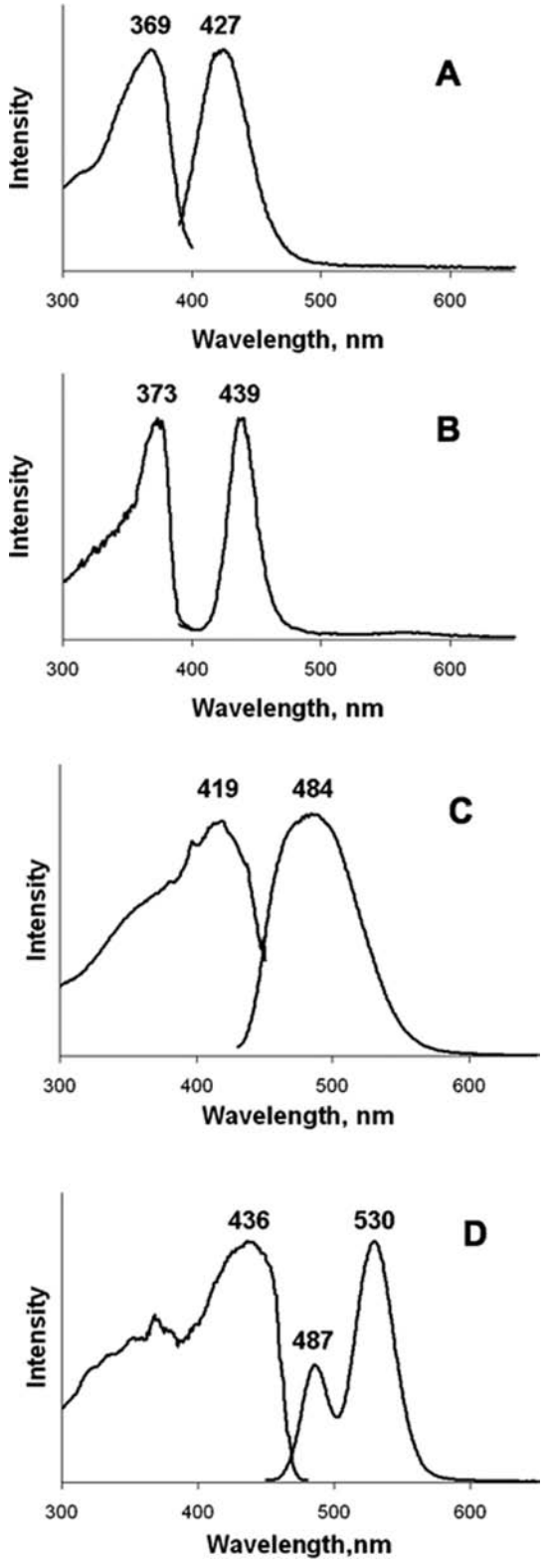

Figure 1. Excitation (left) and emission (right) spectra of the polymorphs of $[(C_6H_{11}NC)_2Au^I](AsF_6)$: (A,B) colorless, blue-glowing polymorph at 298 and 77 K, respectively; (C,D) yellow, green-glowing polymorph at 298 and 77 K, respectively.

$[(C_6H_{11}NC)_2Au^I](PF_6)$. The yellow polymorph of $[(C_6H_{11}NC)_2Au^I](AsF_6)$ crystallizes in the space group $P\bar{1}$ with two halves of cations located on centers of symmetry, another cation in a general position, and two disordered anions in general positions in the asymmetric unit. The cations form kinked chains as seen in Figure 3. The separations between the gold ions are shorter than those found in the colorless polymorph: Au1···Au2, 3.0230(5), Au2···Au3, 3.0097(6) Å. The Au2···Au1···Au2A and Au2···Au3···Au2B angles are required by symmetry to be 180°, while the Au1···Au2···Au3 angle is 154.63(2)°. Again, along the chain of cations, the cyclohexyl groups alternate between axial and equatorial positions. The cyclohexyl groups on the ligands attached to Au2 are in equatorial positions, while the cyclohexyl groups on the ligands attached to Au1 and Au3 are in axial positions.

Figure 4 affords a comparison of the extended chains of cations that are found in the four different types of crystals of $[(C_6H_{11}NC)_2Au^I](PF_6)$ and $[(C_6H_{11}NC)_2Au^I](AsF_6)$.

Concomitant and Controlled Growth of Polymorphs of $[(C_6H_{11}NC)_2Au^I](PF_6)$ and $[(C_6H_{11}NC)_2Au^I](AsF_6)$. The conditions for obtaining these polymorphs have been examined, and the crystallization from dichloromethane/diethyl ether mixtures has been studied in some detail. Figure 5 shows some relevant results obtained by photographing beakers in which crystallization of $[(C_6H_{11}NC)_2Au^I](PF_6)$ occurred. In order to enhance the contrast, these photographs were taken with the sample illuminated by a UV lamp. As the photograph in Figure 5A demonstrates, both polymorphs of $[(C_6H_{11}NC)_2Au^I](PF_6)$ can crystallize concomitantly.[47] Conditions used to obtain this sample are given in the Experimental Section. Alternately, by using a minimal amount of diethyl ether during crystallization, only the colorless, blue-glowing polymorph forms, as shown in Figure 5B. If a large volume of diethyl ether is used and the sample is stirred, then the yellow, greenish-glowing polymorph forms, as shown in Figure 5C.

Figure 6 shows photographs demonstrating that the crystallization of these two polymorphs of $[(C_6H_{11}NC)_2Au^I](PF_6)$ can be spatially controlled. This figure shows pictures of two 5 mm o.d. glass tubes aligned vertically. A sample of $[(C_6H_{11}NC)_2Au^I](PF_6)$ dissolved in dichloromethane was placed in the bottom of each tube. Subsequently, diethyl ether was very carefully layered over each sample. After diffusion of the two phases together, crystallization occurred with the yellow, greenish-glowing polymorph preferentially growing in the upper, diethyl ether-rich section, while the colorless, blue-glowing polymorph formed in the lower, dichloromethane-rich section. These observations are also consistent with the data shown in Figure 5. Similarly, the colorless, blue-glowing polymorph of $[(C_6H_{11}NC)_2Au^I](AsF_6)$ preferentially forms in a dichloromethane-rich environment, while the corresponding yellow, greenish-glowing polymorph forms in a diethyl ether-rich environment.

Vapor-Induced Interconversion of Polymorphs of $[(C_6H_{11}NC)_2Au^I](PF_6)$ and $[(C_6H_{11}NC)_2Au^I](AsF_6)$. Remarkably, exposure of crystals of the yellow, green-glowing polymorph of $[(C_6H_{11}NC)_2Au^I](PF_6)$ or of $[(C_6H_{11}NC)_2Au^I](AsF_6)$ to the vapors of some organic liquids results in their conversion into the colorless, blue-glowing polymorph. Figure 7 shows the effect on a bundle of crystals of $[(C_6H_{11}NC)_2Au^I](AsF_6)$: panels A under ambient light and B under UV irradiation show the sample before exposure to vapor, and panels C and D show the sample after exposure to dichloromethane vapor, which was wafted across the sample from the upper left toward the lower right. As the photographs show, the sample is transformed into blue-glowing material without any detectable change in its external shape.

Table 1. Crystallographic Data for Salts of $[(C_6H_{11}NC)_2Au^I]^+$

	$[(C_6H_{11}NC)_2Au^I](PF_6)$		$[(C_6H_{11}NC)_2Au^I](AsF_6)$	
	yellow polymorph[a]	colorless polymorph[a]	colorless polymorph	yellow polymorph
color/habit	yellow plate	colorless needle	colorless block	yellow-green rod
formula	$C_{14}H_{22}AuF_6N_2P$	$C_{14}H_{22}AuF_6N_2P$	$C_{14}H_{22}AsAuF_6N_2$	$C_{14}H_{22}AsAuF_6N_2$
fw	560.27	560.27	604.22	604.22
crystal system	orthorhombic	monoclinic	monoclinic	triclinic
space group	$P2_12_12_1$	$P2_1/c$	$P2_1/c$	$P\bar{1}$
a, Å	11.5235(7)	6.3644(5)	6.3965(15)	11.7708(12)
b, Å	24.1416(15)	16.9806(15)	17.194(4)	12.4924(13)
c, Å	26.0516(16)	16.7224(13)	16.729(4)	14.783(3)
α, deg	90	90	90	113.248(2)
β, deg	90	92.693(3)	92.658(8)	106.757(2)
γ, deg	90	90	90	91.716(2)
V, Å^3	7247.4(8)	1805.2(3) Å^3	1837.9(7) Å^3	1886.8(5)
Z	16	4	4	4
T, °C	91(2)	91(2)	90(2)	180(2)
λ, Å	0.71073	0.71073	0.71073	0.71073
ρ, g/cm^3	2.054	2.061	2.184	2.127
μ, mm^{-1}	8.264	8.294	9.847	9.592
R_1 (obsd data)[b]	0.055	0.019	0.020	0.057
wR_2 (all data, F_2 refinement)[c]	0.123	0.053	0.050	0.164

[a]Data from ref 33. [b]$R_1 = (\sum||F_o| - |F_c||)/\sum|F_o|$. [c]$wR_2 = ((\sum[w(F_o^2 - F_c^2)^2])/\sum[w(F_o^2)^2])^{1/2}$.

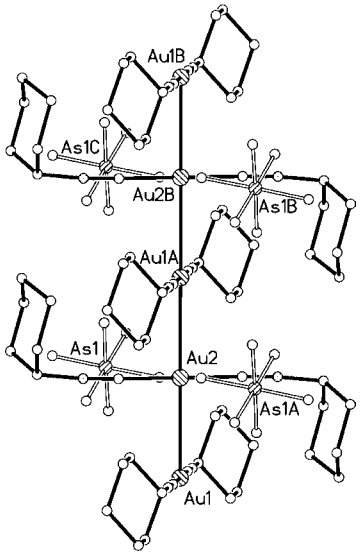

Figure 2. Drawing of a portion of the columnar structure of the colorless polymorph of $[(C_6H_{11}NC)_2Au^I](AsF_6)$. For clarity the atoms are represented by arbitrarily sized circles, and the hydrogen atoms have been omitted. Only four of the five anions are shown.

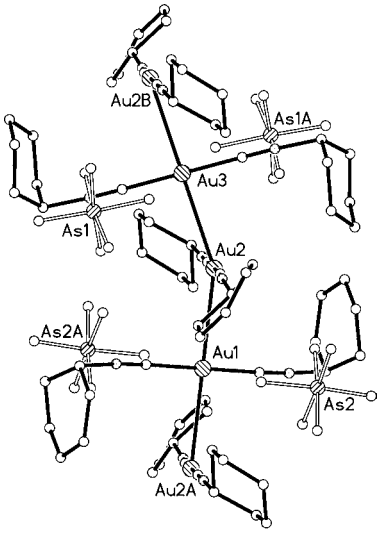

Figure 3. Drawing of a portion of the chain of cations in the yellow polymorph of $[(C_6H_{11}NC)_2Au^I](AsF_6)$. For clarity, the atoms are represented by arbitrarily sized circles, and the hydrogen atoms have been omitted. Only four of the five anions are shown.

Figure 8 shows that the transformation is not simply occurring on the surface. Again we start with the sample of yellow, green-glowing polymorph of $[(C_6H_{11}NC)_2Au^I](AsF_6)$ under ambient light (Figure 8A) and under UV irradiation (Figure 8B). After exposure to dichloromethane vapor, the sample is partially converted into the blue-glowing polymorph as shown in Figure 8C. Crushing this blue-glowing tip of this sample reveals that the transformation has not just altered the surface but has penetrated into the bulk of the sample.

Similar behavior is also shown by the yellow, green-glowing polymorph of $[(C_6H_{11}NC)_2Au^I](PF_6)$. Figure 9 shows photographs taken from a sample in which a bundle of yellow crystals of $[(C_6H_{11}NC)_2Au^I](PF_6)$ was cemented into a hole on a glass box with vacuum grease. Dichloromethane vapor was added to the inside of the box. The photograph shows the sample with the lower part inside the box and the upper part protruding outside the box. As time passes and vapor exposure continues inside the box, the sample gradually is transformed from green-glowing to blue-glowing. The portion of the sample outside the box is also affected, and it appears that the transformation is progressing along the bundle from inside to outside.

The transformation of the yellow, green-glowing polymorph of $[(C_6H_{11}NC)_2Au^I](PF_6)$ into the colorless, blue-glowing form has also been monitored by X-ray powder diffraction as shown in Figure 10. The powder patterns of yellow, green-glowing polymorph of $[(C_6H_{11}NC)_2Au^I](PF_6)$ are shown in traces A and B. Trace A shows the pattern computed from the single crystal diffraction data, while trace B shows the

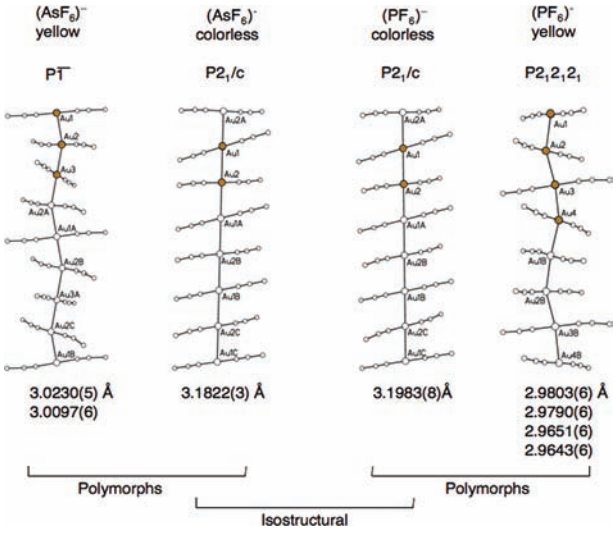

Figure 4. Drawing comparing the chains of cations found in the polymorphs of $[(C_6H_{11}NC)_2Au^I](AsF_6)$ and $[(C_6H_{11}NC)_2Au^I](PF_6)$. For clarity, only one carbon atom of each cyclohexyl ring is shown and the anions are omitted.

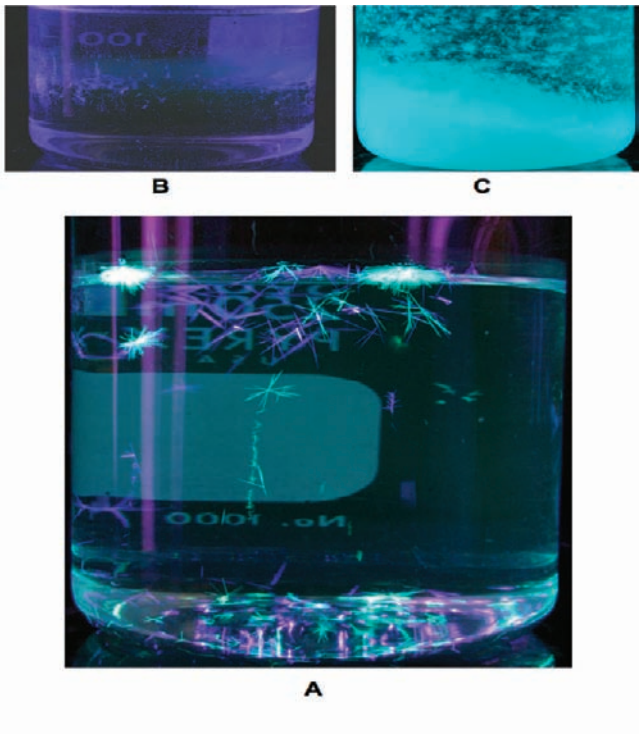

Figure 5. Crystallization of $[(C_6H_{11}NC)_2Au^I](PF_6)$ from dichloromethane/diethyl ether mixtures: (A) concomitant crystallization of colorless, blue-glowing and yellow, green-glowing crystals; (B) exclusive formation of colorless, blue-glowing polymorph; (C) exclusive formation of the yellow, green-glowing polymorph produced by stirring the mixture.

experimental data for the yellow, green-glowing polymorph. After exposure of the sample in trace B to dichloromethane vapor, the data in trace C were obtained. Comparison of the data in trace C with those obtained from a sample of the colorless, blue-glowing polymorph of $[(C_6H_{11}NC)_2Au^I](PF_6)$ presented in trace D show that the conversion occurs without the net uptake of any vapor.

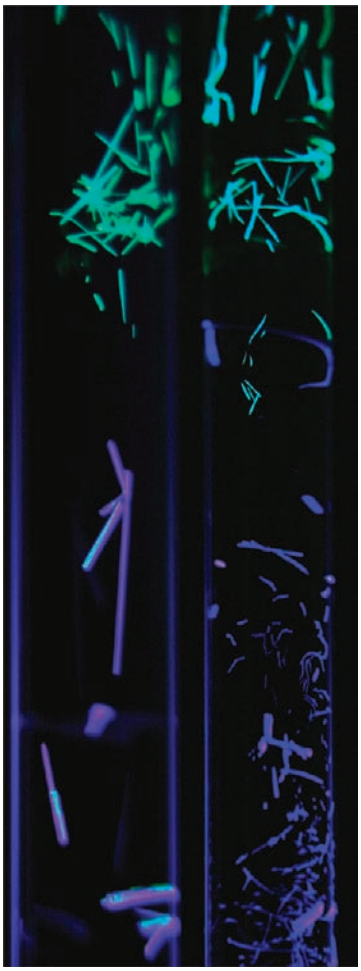

Figure 6. Photographs demonstrating spatially separated crystallization of the colorless, blue-glowing and yellow, green-glowing crystals of $[(C_6H_{11}NC)_2Au^I](PF_6)$ in two 5 mm o.d. glass tubes. The complex was dissolved in dichloromethane and placed at the bottom of each tube. Subsequently, diethyl ether was very carefully layered over the dichloromethane solution and the mixture allowed to stand undisturbed.

Dichloromethane vapor is not the only gas that can convert the yellow, green-glowing polymorphs into their colorless, blue-glowing counterparts. Exposures to vapors of acetone, methanol, or acetonitrile also cause this transformation. On the other hand, the vapors of diethylether, water, or pentane do not produce any change to the yellow, green-glowing polymorphs. Notice the parallels here with the crystal growth experiments. The yellow, green-glowing polymorphs grew in diethyl ether-rich regions, and diethyl ether vapor has no affect on this polymorph. On the other hand, the colorless, blue-glowing form grew in dichloromethane-rich regions, and dichloromethane vapor converts the yellow, green-glowing polymorph into the colorless, blue-glowing polymorph.

Thermally Induced Interconversion of Polymorphs of $[(C_6H_{11}NC)_2Au^I](AsF_6)$. Upon heating, the colorless, blue-emitting polymorph of $[(C_6H_{11}NC)_2Au^I](AsF_6)$ is transformed into a yellow solid, without melting over the temperature range, 98−102 °C. Figure 11A, B shows the luminescence spectra of a sample of the colorless polymorph after heating to 120 °C and then cooling the sample. Comparison of these two spectra with the spectra in Figure 1, shows that the heat treated sample has the same emission characteristics as the yellow, green-emitting

dx.doi.org/10.1021/ja302025m | J. Am. Chem. Soc. 2012, 134, 10885−10893

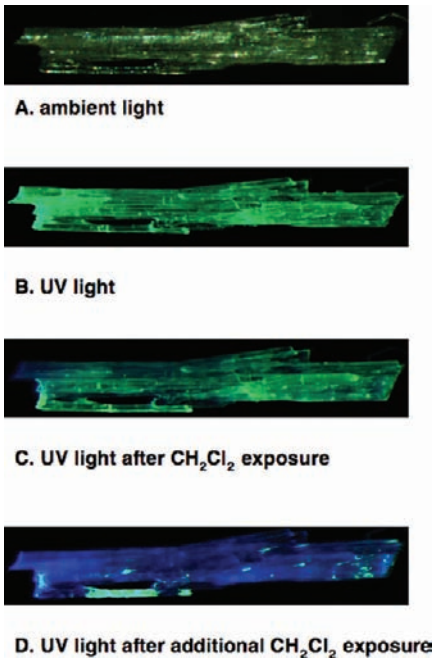

Figure 7. Photographs of crystals of $[(C_6H_{11}NC)_2Au^I](AsF_6)$: (A) under ambient light, (B) under UV irradiation, (C) after exposure to dichloromethane vapor under UV irradiation, and (D) after additional exposure to dichloromethane vapor under UV irradiation.

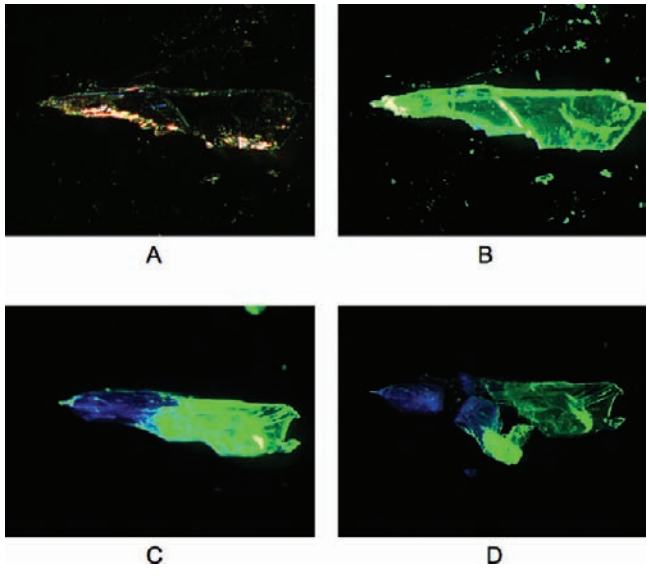

Figure 8. Photographs of crystals of $[(C_6H_{11}NC)_2Au^I](AsF_6)$: (A) under ambient light, (B) under UV irradiation, (C) after exposure to dichloromethane vapor under UV irradiation, and (D) after crushing the crystal under UV irradiation.

polymorph of $[(C_6H_{11}NC)_2Au^I](AsF_6)$. X-ray powder diffraction (see Supporting Information) also confirms that heating the colorless solid to 120 °C without melting results in its transformation into the yellow, green-emitting polymorph. Further heating of this sample results in melting over the temperature range 123−125 °C to give a colorless, luminescent melt. Upon cooling the melt, a yellow solid is formed. As the emission spectra shown in Figure 11C, D reveal, the emission of the material at this stage does not correspond to the spectra of either the colorless or the yellow polymorph. However, after

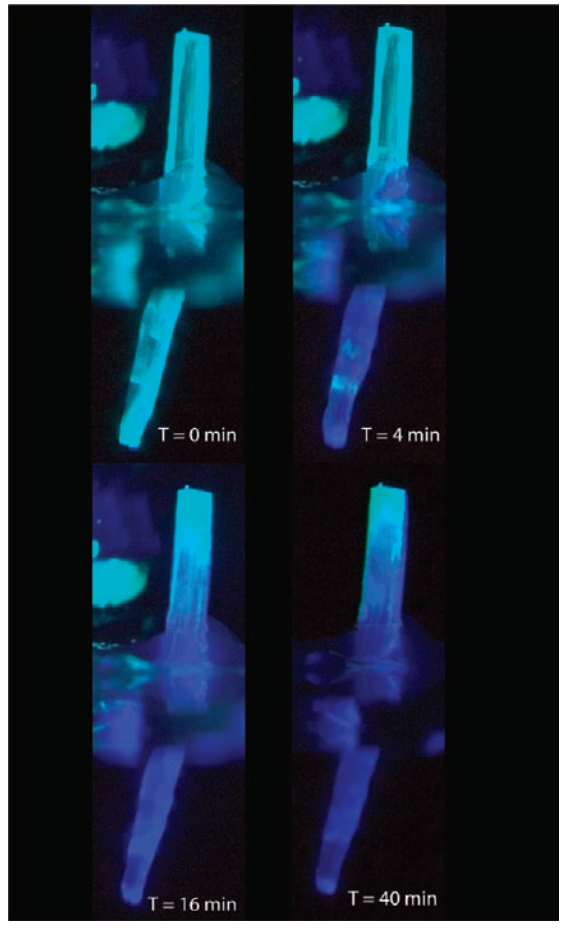

Figure 9. Photographs of a bundle of crystals of $[(C_6H_{11}NC)_2Au^I](PF_6)$ at various times after exposure to dichloromethane vapor. The lower part of the bundle is inside a box where dichloromethane vapor is present, while the top part of the bundle is outside the box.

standing for 24 h, the emission spectrum of the sample changes into that of the yellow, green-emitting polymorph as seen in the data in Figure 11E, F. Attempts to obtain X-ray powder diffraction from the sample used to generate the spectra shown in Figure 11C, D were not successful. Thus, this metastable solid appears to be amorphous, not crystalline.

Heating the yellow polymorph results in its melting over the temperature range 123−126 °C to produce a colorless, luminescent melt. This behavior is consistent with the observations on heating the colorless polymorph to produce the yellow phase that melted at 123−125 °C.

The polymorphs of $[(C_6H_{11}NC)_2Au^I](PF_6)$ do not undergo an analogous phase change. As reported earlier, the colorless polymorph melts over the temperature range 115−120 °C, while the yellow polymorph melts over the range, 110−115 °C.[33] Both yield a colorless melt with a bluish emission and form the yellow polymorph upon cooling.

■ DISCUSSION

The crystallographic data for the yellow and colorless forms of $[(C_6H_{11}NC)_2Au^I](AsF_6)$ show that they are true polymorphs that are free of any sort of solvate inclusion. Similar considerations hold for the yellow and colorless forms of $[(C_6H_{11}NC)_2Au^I](PF_6)$. Remarkably, the yellow polymorphs of $[(C_6H_{11}NC)_2Au^I](AsF_6)$ and $[(C_6H_{11}NC)_2Au^I](PF_6)$ are not isostructural, but crystallize in different space groups and

dx.doi.org/10.1021/ja302025m | J. Am. Chem. Soc. 2012, 134, 10885−10893

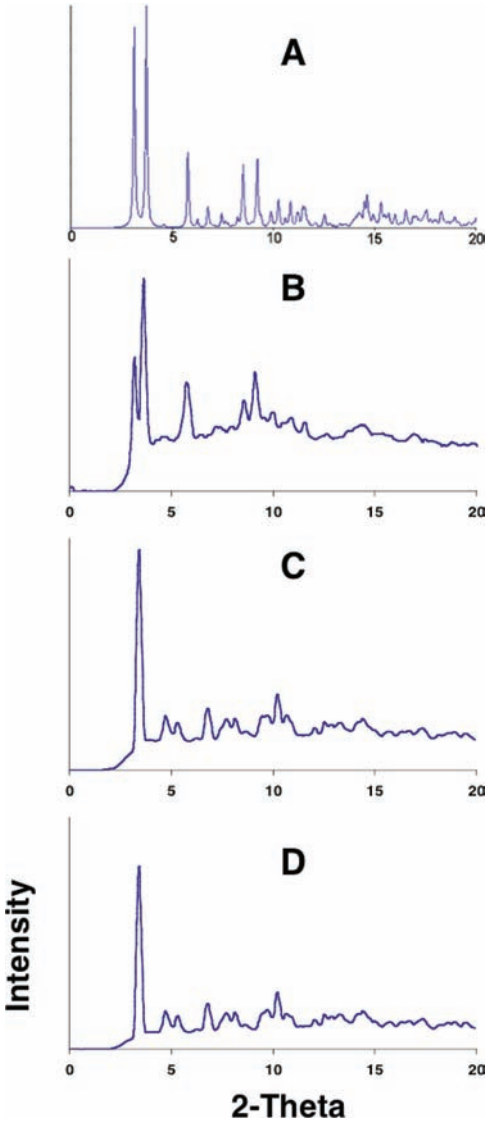

Figure 10. Powder X-ray diffraction data for $[(C_6H_{11}NC)_2Au^I](PF_6)$. (A) Computed pattern from the single crystal data for the yellow polymorph. (B) Experimental data from the yellow polymorph. (C) Observed diffraction from the same sample after exposure to dichloromethane vapor. (D) Experimental data from the colorless polymorph.

have differences in the nature of self-association in the columns of cations as best seen in Figure 4. On the other hand, the colorless, blue-emitting polymorphs are isostructural with the most significant difference occurring in the Au···Au separation. That separation is larger for the colorless form of $[(C_6H_{11}NC)_2Au^I](AsF_6)$ which has the larger anion. Likewise, the Au···Au separations are slightly longer in the yellow polymorph of $[(C_6H_{11}NC)_2Au^I](AsF_6)$ than in the yellow polymorph of $[(C_6H_{11}NC)_2Au^I](PF_6)$.

Among the four structures of $[(C_6H_{11}NC)_2Au^I](AsF_6)$ and $[(C_6H_{11}NC)_2Au^I](PF_6)$, it is interesting to compare the axial/equatorial orientations of the cyclohexyl rings along each chain. Each cation in all four different types of crystals is coordinated by two cyclohexylisocyanide ligands that share the same conformation of the cyclohexyl group. Thus, there are two types of cations: one with both the isocyano groups in axial positions of the cyclohexyl rings, the other with the isocyano

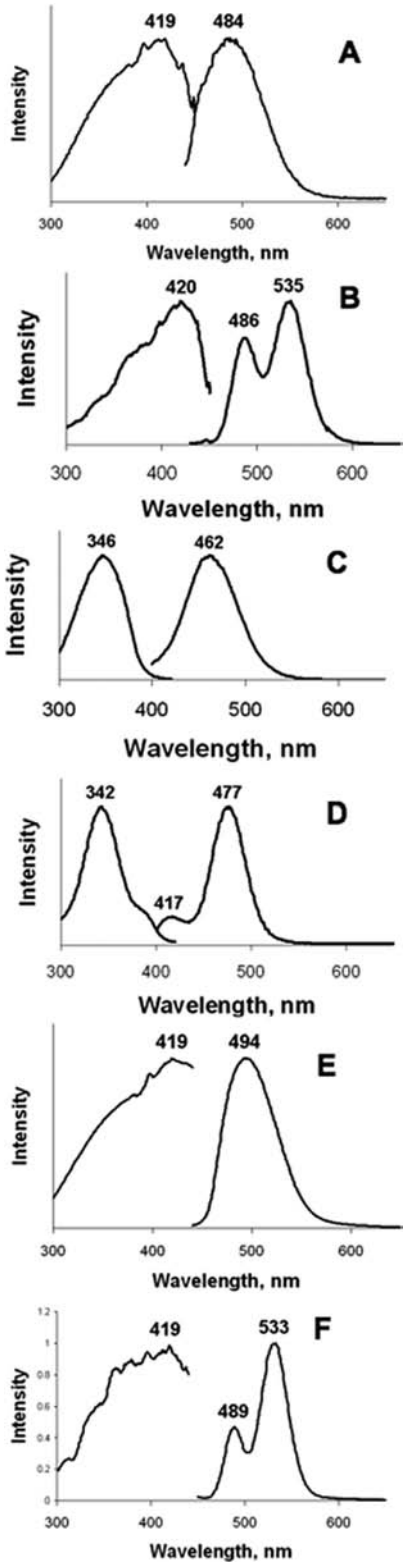

Figure 11. Excitation (left) and emission (right) spectra the colorless, blue-glowing polymorph of $[(C_6H_{11}NC)_2Au^I](AsF_6)$: (A, B) after heating to 393 K and cooling to 298 and 77 K, respectively; (C, D) after melting at 403−406 K and immediately cooling to 298 and 77 K, respectively; (E, F) the same sample used to obtain the spectra in panels C and D after standing at 298 K for 24 h, recorded at 298 and 77 K, respectively.

dx.doi.org/10.1021/ja302025m | J. Am. Chem. Soc. 2012, 134, 10885−10893

groups in equatorial positions in the cyclohexyl ring. These two types of cations alternate along any of the chains found in the four crystalline materials discussed here. In these crystals, none of the cations has one isocyano group in an equatorial position and the other in an axial position.

Although the yellow polymorphs of $[(C_6H_{11}NC)_2Au^I](AsF_6)$ and $[(C_6H_{11}NC)_2Au^I](PF_6)$ differ in their structures, both are sensitive to the vapors of certain volatile organic compounds and undergo a vapor-induced transformation into the respective colorless, blue-emitting polymorph. This transformation occurs throughout the crystal, although it appears to originate on the surface. Thus, finely ground samples respond much more rapidly to the presence of vapor than do large crystals. While transient absorption of the vapor onto the surface of the crystals may occur during the phase transition, there is no net uptake of molecules of vapor into these crystals. Thus, the vapor-triggered process reported here differs markedly from those of other vapochromic and vapoluminescent materials where vapor is incorporated into the crystals and their composition changes. In regard to these transformations, additional studies are in progress to better understand the mechanism involved. The alternating axial/equatorial orientation of the cyclohexyl rings along each chain may provide a domino-like mechanism that allows reorientation of the individual cations in the yellow polymorph when vapor interacts with the crystal surface.

Since the polymorphs of $[(C_6H_{11}NC)_2Au^I](AsF_6)$ and $[(C_6H_{11}NC)_2Au^I](PF_6)$ are intensely luminescent, their reactions are readily monitored, particularly by the human eye. Other vapor-related polymorphic phase changes could easily go unnoticed in nonluminescent crystals and could contribute to the difficulties encountered in regard to polymorph formation (disappearing polymorphs) and stability.[48] Control of polymorph stability is a significant feature in any technological process that utilizes chemicals in crystalline form and is a particular issue for drug development, since many drugs are prepared and used in solid form.[30,31,49,50]

■ CONCLUSIONS

We have examined aspects of the crystallization of polymorphs of $[(C_6H_{11}NC)_2Au^I](AsF_6)$ and $[(C_6H_{11}NC)_2Au^I](PF_6)$ and documented the remarkable, vapor-induced conversion of the yellow, green-glowing polymorphs, each with a different crystallographic structure, into the corresponding colorless, blue-emitting polymorph.

■ EXPERIMENTAL SECTION

Materials. Isocyanides are toxic and foul smelling and need to be handled appropriately. All reactions were carried out in the atmosphere at room temperature in a well-ventilated hood. Samples of cyclohexyl isocyanide were purchased from Aldrich and used as received. Chloro(tetrahydrothiophene)gold(I) was prepared by an established method.[51]

Preparation of $[(C_6H_{11}NC)_2Au^I](AsF_6)$. A 25 mL beaker was charged with 0.275 g (0.858 mmol) of chloro(tetrahydrothiophene)-gold(I), 0.187 g (1.71 mmol) of cyclohexyl isocyanide, and 5 mL of acetonitrile while stirring. Once the mixture became homogeneous (after ∼10 min), 0.170 g (0.868 mmol) of lithium hexafluoroarsenate in 8 mL of acetonitrile was added. The combined mixture was stirred for 30 s and filtered, and volatiles were removed by rotary evaporation. The residue was dissolved in 5 mL of dichloromethane, and the resulting solution was filtered through a short pad of Celite. Diethyl ether was then added to precipitate 0.424 g (0.702 mmol) of $[(C_6H_{11}NC)_2Au^I](AsF_6)$ as a colorless solid (82%). To obtain the yellow-green polymorph of $[(C_6H_{11}NC)_2Au^I](AsF_6)$, 0.100 g (0.165 mmol) of either white or yellow-green $[(C_6H_{11}NC)_2Au^I](AsF_6)$ was dissolved in 0.4 mL of dichloromethane. A copious amount of diethyl ether (∼40 mL) was then rapidly added to the colorless solution, immediately producing a white microcrystalline solid that turns yellow-green upon standing. However, gently rubbing the flask's sides with a wooden applicator stick after the addition of diethyl ether promotes the rapid formation of the yellow-green polymorph while reducing the formation of the colorless polymorph. To obtain the colorless polymorph of $[(C_6H_{11}NC)_2Au](AsF_6)$, 0.100 g (0.165 mmol) of either white or yellow-green $[(C_6H_{11}NC)_2Au](AsF_6)$ was dissolved in 3 mL of dichloromethane, followed by the slow addition of diethyl ether until colorless needles started to form. Swirling the flask and slow addition of more diethyl ether helps ensure complete crystallization of the colorless polymorph. ^1H NMR (400 MHz, $CDCl_3$, 25 C): δ = 4.11 (m, 2H), 2.00 (m, 4H), 1.77 (m, 4H), 1.66 (m, 4H), 1.44 (m, 4H), 1.41 (m, 4H). $^{13}C\{^1H\}$ NMR (100 MHz, $CDCl_3$, 25 °C): δ = 138.4, 55.9, 31.2, 24.4, 22.6. UV (CH_2Cl_2) λ_{max}, nm (ε): 216 (9543), 238 (3068), 244 (3386). IR: yellow-green polymorph, 2969, 2947, 2943, 2879, 2865, 2841, 2262 cm^{-1}; colorless polymorph, 2970, 2884, 2846, 2835, 2270, 2257 cm^{-1}.

Production of the Mixture of Blue and Green Luminescent Crystals of $[(C_6H_{11}NC)_2Au](PF_6)$ Shown in Figure 5A. A 0.238 g (0.425 mmol) sample of $[(C_6H_{11}NC)_2Au](PF_6)$ was placed in a 250 mL beaker with 5 mL of dichloromethane. A 15 mL portion of diethyl ether was added to this colorless, nonluminescent solution, whereupon a luminescent haze formed. Swirling the beaker removed this haze and the luminescence associated with it. An additional 10 mL of diethyl ether was added to produce this luminescent haze that disappeared with gentle swirling of the flask. The process was repeated once more using 5 mL of diethyl ether. Then, very gently, ∼120 mL of diethyl ether was layered over the dichloromethane/diethyl ether solution. This addition produced a 3/4 in. wide band with a bluish/green luminescent haze in between these layers. Within this band both blue-glowing and green-glowing crystals formed. As the layers began to diffuse together over the next 15 min, blue-glowing and green-glowing crystals started to form in all regions of the beaker.

Production of the Blue Luminescent Crystals of $[(C_6H_{11}NC)_2Au](PF_6)$ Shown in Figure 5B. A 0.250 g (0.446 mmol) sample of $[(C_6H_{11}NC)_2Au](PF_6)$ was placed in a 250 mL beaker with 6 mL of dichloromethane. A 15 mL portion of diethyl ether was added to this colorless, nonluminescent solution, whereupon a luminescent haze formed. Swirling the beaker removes this haze and the luminescence associated with it. An additional 15 mL of diethyl ether was again added to produce this luminescent haze that again went away with gentle swirling of the flask. The process was repeated twice more using 5 mL of diethyl ether at each addition. At this point small, blue luminescent crystals began to form in the beaker. A final addition of ∼35 mL of diethyl ether was made, and the entire contents of the beaker were allowed to stand for several minutes, whereupon larger blue luminescent crystals formed.

Production of the Green Luminescent Microcrystalline $[(C_6H_{11}NC)_2Au](PF_6)$ Shown in Figure 5C. A 0.148 g (0.264 mmol) sample of $[(C_6H_{11}NC)_2Au](PF_6)$ was placed in a 250 mL beaker with 1 mL of dichloromethane. To this colorless, non-luminescent solution was rapidly added 200 mL of diethyl ether, whereupon a green luminescent haze formed. Rapid stirring of this mixture with a wooden applicator stick produced a microcrystalline, green luminescent solid. After approximately 5 min no other solid material formed. Careful inspection of the bulk material showed no contamination of the blue luminescent polymorph. If after the green luminescent haze formed, no rapid stirring took place, larger green luminescent crystals began to form. However, small amounts of blue luminescent crystals also formed alongside these green luminescent crystals.

X-ray Crystallography and Data Collection. The crystals were removed from the source together with a small amount of mother liquor and immediately coated with a hydrocarbon oil on the microscope slide. A suitable crystal of each compound was mounted on a glass fiber with silicone grease and placed in the cold stream of a

Bruker SMART CCD with graphite-monochromated Mo Kα radiation. Crystal data are given in Table 1.

The structures were solved by direct methods and refined with all data (based on F^2) using the software of SHELXTL 5.1. A multiscan method utilizing equivalents was employed to correct for absorption.[52] Hydrogen atoms were added geometrically and refined with a riding model.

Physical Measurements. Infrared spectra were recorded as pressed KBr pellets on a Matteson Galaxie Series FTIR 3000 spectrometer. Electronic absorption spectra were recorded using a Hewlett-Packard 8450A diode array spectrophotometer. Fluorescence excitation and emission spectra were recorded on a Jobin Yvon Fluoromax-P luminescence spectrophotometer.

■ ASSOCIATED CONTENT

Supporting Information

Figures SI-1−SI-7, showing X-ray powder diffraction data for the yellow and colorless polymorphs; X-ray crystallographic files in CIF format for the colorless and yellow polymorphs of $[(C_6H_{11}NC)_2Au](AsF_6)$. This material is available free of charge via the Internet at http://pubs.acs.org.

■ AUTHOR INFORMATION

Corresponding Author

albalch@ucdavis.edu

Notes

The authors declare no competing financial interest.

■ ACKNOWLEDGMENTS

We thank the donors of the Petroleum Research Fund (Grants 37056 and 40030) for support. The Bruker SMART 1000 diffractometer was funded in part by NSF Instrumentation grant CHE-9808259.

■ REFERENCES

(1) Zhao, Q.; Li, F.; Huang, C. *Chem. Soc. Rev.* **2010**, *39*, 3007−3030.
(2) Fiddler, M. N.; Begashaw, I.; Mickens, M. A.; Collingwood, M. S.; Assefa, Z.; Bililign, S. *Sensors* **2009**, *9*, 10447−10512.
(3) He, X.; Yam, V. W. *Coord. Chem. Rev.* **2011**, *255*, 2111−2123.
(4) Fernández, E. J.; López-de-Luzuriaga, J. M.; Monge, M.; Olmos, M. E.; Pérez, J.; Laguna, A.; Mohamed, A. A.; Fackler, J. P., Jr. *J. Am. Chem. Soc.* **2003**, *125*, 2022−2023.
(5) Fernández, E. J.; López-de-Luzuriaga, J. M.; Monge, M.; Montiel, M.; Olmos, M. E.; Pérez, J.; Laguna, A.; Mendizabal, F.; Mohamed, A. A.; Fackler, J. P., Jr. *Inorg. Chem.* **2004**, *43*, 3573−3581.
(6) Lasanta, T.; Olmos, M. E.; Laguna, A.; López-de-Luzuriaga, J. M.; Naumov, P. *J. Am. Chem. Soc.* **2011**, *133*, 16358−16361.
(7) Laguna, A.; Lasanta, T.; López-de-Luzuriaga, J. M.; Monge, M.; Naumov, P.; Olmos, M. E. *J. Am. Chem. Soc.* **2010**, *132*, 456−457.
(8) Strasser, C. E.; Catalano, V. J. *J. Am. Chem. Soc.* **2010**, *132*, 10009−10011.
(9) Kunugi, Y.; Mann, K. R.; Miller, L. L.; Exstrom, C. L. *J. Am. Chem. Soc.* **1998**, *120*, 589−590.
(10) Daws, C. A.; Exstrom, C. L.; Sowa, J. R.; Mann, K. R. *Chem. Mater.* **1997**, *9*, 363−368.
(11) Kunugi, Y.; Miller, L. L.; Mann, K. R.; Pomije, M. K. *Chem. Mater.* **1998**, *10*, 1487−1489.
(12) Exstrom, J. M.; Sowa, J., J. R.; Daws, C. A.; Janzen, D.; Mann, K. R. *Chem. Mater.* **1995**, *7*, 15−17.
(13) Buss, C. E.; Anderson, C. E.; Pomije, M. K.; Lutz, C. M.; Britton, D.; Mann, K. R. *J. Am. Chem. Soc.* **1998**, *120*, 7783−7790.
(14) Buss, C. E.; Mann, K. R. *J. Am. Chem. Soc.* **2002**, *124*, 1031−1039.
(15) Grove, L. J.; Rennekamp, J. M.; Jude, H.; Connick, W. B. *J. Am. Chem. Soc.* **2004**, *126*, 1594−1595.
(16) Kobayashi, A.; Dosen, M.; Chang, M.; Nakajima, K.; Noro, S.; Kato, M. *J. Am. Chem. Soc.* **2010**, *132*, 15286−15298.
(17) Chang, M.; Kobayashi, A.; Nakajima, K.; Chang, H.-C.; Kato, M. *Inorg. Chem.* **2011**, *50*, 8308−8317.
(18) Ford, P. C.; Cariati, E.; Bourassa, J. *Chem. Rev.* **1999**, *99*, 3625−3647.
(19) Cariati, E.; Bourassa, J.; Ford, P. C. *J. Chem. Soc., Chem. Commun.* **1998**, 1623−1624.
(20) Balch, A. L. *Struct. Bonding (Berlin)* **2007**, *123*, 1−40.
(21) Schmidbaur, H.; Schier, A. *Chem. Soc. Rev.* **2012**, *41*, 370−412.
(22) Pyykkö, P. *Chem. Soc. Rev.* **2008**, *37*, 1967−1997.
(23) Bernstein, J. *Polymorphism in Molecular Crystals*; Clarendon Press: Oxford, 2002.
(24) Dunitz, J. D.; Bernstein, J. *Acc. Chem. Res.* **1995**, *28*, 193−200.
(25) Braga, D.; Grepioni, F. *Chem. Soc. Rev.* **2000**, *29*, 229−238.
(26) Olmstead, M. M.; Jiang, F.; Balch, A. L. *Chem. Commun.* **2000**, 483−484.
(27) Bernstein, J. *J. Phys. D: Appl. Phys* **1993**, *26*, 666−876.
(28) Kistenmacher, T. J.; Emge, T. J.; Bloch, A. N.; Cowan, D. O. *Acta Crystallogr. Sect. B: Struct. Sci.* **1982**, *B38*, 1193−1199.
(29) Bechgaard, K.; Kistenmacher, T. J.; Bloch, A. N.; Cowan, D. O. *Acta Crystallogr. Sect. B: Struct. Sci.* **1977**, *B33*, 417−422.
(30) Gardner, C. R.; Walsh, C. T.; Almarsson, Ö. *Nature Rev. Drug Discov.* **2004**, *3*, 926−934.
(31) Datta, S.; Grant, D. J. W. *Nature Rev. Drug Discov.* **2004**, *3*, 42−57.
(32) Chemburkar, S. R.; John Bauer, J.; Deming, K.; Spiwek, H.; Patel, K.; Morris, J.; Henry, R.; Spanton, S.; Dziki, W.; Porter, W.; Quick, J.; Bauer, P.; Donaubauer, J.; Narayanan, B. A.; Soldani, M.; Riley, D.; McFarland, K. *Org. Process Res. Dev.* **2000**, *4*, 413−417.
(33) White-Morris, R. L.; Olmstead, M. M.; Balch, A. L. *J. Am. Chem. Soc.* **2003**, *125*, 1033−1040.
(34) (a) Toronto, D. V.; Weissbart, B.; Tinti, D. S.; Balch, A. L. *Inorg. Chem.* **1996**, *35*, 2484−2489. (b) Weissbart, B.; Toronto, D. V.; Balch, A. L.; Tinti, D. S. *Inorg. Chem.* **1996**, *35*, 2490−2496.
(35) Weissbart, B.; Toronto, D. V.; Balch, A. L.; Tinti, D. S. *Inorg. Chem.* **1996**, *35*, 2490−2496.
(36) Balch, A. L. *Gold Bull.* **2004**, *37*, 45.
(37) Lefebvre, J.; Batchelor, R. J.; Leznoff, D. B. *J. Am. Chem. Soc.* **2004**, *126*, 16117−16125.
(38) Katz, M. J.; Ramnial, T.; Yu, H.-Z.; Leznoff, D. B. *J. Am. Chem. Soc.* **2008**, *130*, 10662−10673.
(39) White-Morris, R. L.; Olmstead, M. M.; Attar, S.; Balch, A. L. *Inorg. Chem.* **2005**, *44*, 5021−5029.
(40) Gussenhoven, E. M.; Fettinger, J. C.; Pham, D. M.; Malwitz, M. A.; Balch, A. L. *J. Am. Chem. Soc.* **2005**, *127*, 10838.
(41) Manbeck, G. F.; Brennessel, W. W.; Stockland, R. A., Jr.; Eisenberg, R. *J. Am. Chem. Soc.* **2010**, *132*, 12307−12318.
(42) Lim, S. H.; Olmstead, M. M.; Fettinger, J. C.; Balch, A. L. *Inorg. Chem.* **2012**, *51*, 1925−1932.
(43) Mansour, M. A.; Connick, W. B.; Lachicotte, R. J.; Gysling, H. J.; Eisenberg, R. *J. Am. Chem. Soc.* **1998**, *120*, 1329−1330.
(44) Lee, Y. A.; McGarrah, J. E.; Lachicotte, R. J.; Eisenberg, R. *J. Am. Chem. Soc.* **2002**, *124*, 10662−10663.
(45) Han, S.; Yoon, Y. Y.; Jung, O.-S.; Lee, Y. A. *Chem. Commun.* **2011**, *47*, 10689−10691.
(46) Parks, J. E.; Balch, A. L. *J. Organomet. Chem.* **1974**, *71*, 453.
(47) Bernstein, J.; Davey, R. J.; Henck, J. O. *Angew. Chem., Int. Ed.* **1999**, *38*, 3440−3461.
(48) Lancaster, R. W.; Harris, L. D.; Pearson, D. *CrystEngComm* **2011**, *13*, 1775−1777.
(49) Blagden, N.; Davey, R. J. *Cryst. Growth Des.* **2003**, *3*, 873−885.
(50) Davey, R. J. *Chem. Commun.* **2003**, 1463−1467.
(51) Bruce, M. I.; Nicholson, B. K.; Bin Shawkataly, O. *Inorg. Synth.* **1989**, *26*, 325.
(52) Sheldrick, G. M. *SADABS 2.0*, based on a method of Blessing, R. H. *Acta Crystallogr., Sect. A* **1995**, *A51*, 33.